Journal of Imaging Science and Technology® 50(1): 64–72, 2006.

Multispectral Image Compression for High Fidelity Colorimetric and Spectral Reproduction

Shanshan Yu
Imaging Science and Engineering Lab, Tokyo Institute of Technology, Japan
E-mail: yss@isl.titech.ac.jp

Yuri Murakami
Frontier Collaborative Research Center, Tokyo Institute of Technology, Japan
and Akasaka Natural Vision Research Center, NICT, Japan

Takashi Obi
Interdisciplinary Graduate School of Science and Engineering, Tokyo Institute of Technology, Japan

Masahiro Yamaguchi
Imaging Science and Engineering Lab, Tokyo Institute of Technology, Japan
and Akasaka Natural Vision Research Center, NICT, Japan

Nagaaki Ohyama
Frontier Collaborative Research Center, Tokyo Institute of Technology, Japan
and Akasaka Natural Vision Research Center, NICT, Japan

Abstract. *The article aims to provide a solution for multispectral image compression for high color reproducibility with preservation to spectral accuracy. In the method previously proposed to reduce the colorimetric error of the reconstructed multispectral image, a weighting matrix is incorporated to Karhunen-Loeve transform (KLT) as the spectral transform for multispectral image compression, which accounts for the color matching functions of human observers as well as the viewing illuminants. However, the colorimetric improvements are obtained on the cost of degradation of spectral accuracy. In this paper, we show that the reduction of colorimetric error and the preservation of spectral accuracy is a tradeoff that can be controlled by adding a diagonal matrix that is composed of a scalar multiple of an identity matrix to the weighting matrix of KLT. As the result, the small values in the weighting matrix can be lifted up, thus reduce the spectral errors in the corresponding reconstructed multispectral image bands. We implement a multispectral image compression system that integrates the proposed spectral transforms with the addition of diagonal matrix and JPEG2000 for high colorimetric and spectral reproducibility. Experimental results for three 16-band multispectral images show that spectral accuracy can be improved without loss of substantial color reproducibility if the magnitude of the scalar in the diagonal matrix is chosen appropriately © 2006 Society for Imaging Science and Technology.*
[DOI: 10.2352/J.ImagingSci.Technol.(2006)50:1(64)]

INTRODUCTION

Multispectral imaging (MSI) is a promising technology for critical color-matching applications such as telemedicine, electronic museum, art book reproductions, on-line shopping, etc., since conventional RGB color images, although pleasing, are unacceptable in respect for high fidelity color reproduction.[1,2] In response to the huge data volume of multispectral images, many compression algorithms have been carried for the efficiency of transmission, mainly in the field of remote sensing.[3,4] Among various methods, transform coding based methods are one of the feasible solutions for multispectral image compression. When multispectral images are coded by transform coding, spectral and spatial transforms are usually independently and sequentially applied.[5] A typical multispectral image compression system is composed of Karhunen-Loeve transform (KLT) as the spectral transform and discrete cosine transform (DCT) or discrete wavelet transform (DWT) as the spatial ones, followed by quantization and encoding.

However, these conventional transforms of multispectral image compression are mostly designed for better spectral accuracy purpose and use mean squared error (MSE) based evaluation measurements, e.g., peak signal-to-noise ratio (PSNR). That is to say, they aim to minimize the difference between the original and reconstructed multispectral images. In the applications for color reproduction, it is valuable to utilize the characteristics of visual color perception, but conventional compression methods do not take the advantage of colorimetry into consideration. In response to this problem, Murakami used a method called weighted KLT (WKLT) as the spectral transform for multispectral image compression,[6] which is a special case of one mode analysis (OMA).[7] In this method, the colorimetric error is decreased as compared to conventional KLT based methods by incorporating a weighting matrix to KLT that accounts for the color matching functions of human observer. Mase com-

Received Jan. 31, 2005; accepted for publication Sep. 25, 2005.
1062-3701/2006/50(1)/64/9/$20.00.

bined WKLT with JPEG2000 as the spatial compression scheme for multispectral image compression and confirmed the effectiveness of WKLT in the aspect to reduce color difference in CIE L*a*b* color space.[8]

However, the improvements in color reproduction for OMA and WKLT based compression schemes are obtained on the cost of poor spectral accuracy in certain wavelengths. In some applications, multispectral imaging technology is valuable for both accurate color reproduction and spectral image analysis, for example, medical color imaging, textile, and other merchandize imaging for electronic commerce and digital archive of historical artworks. In those applications, spectral information is used for classification,[9] recognition,[10] material identification,[11] and content-based image retrieval.[12] In addition, in printer industry, spectral transmittance images are required for the spectral reproduction techniques.[13] In these occasions, the loss of spectral accuracy is not expected. In this paper, we show that the preservation of spectral accuracy and the reduction of colorimetric error is a tradeoff, which can be controlled by adding a diagonal matrix that is composed of a scalar multiple of an identity matrix to the weighting matrix of KLT. It is also demonstrated that spectral accuracy can be improved without substantial colorimetric degradation if the scalar is chosen appropriately.

In order to evaluate the performance of the addition of diagonal matrix to the weighting matrix, we use the following spectral transforms for multispectral image compression: KLT, WKLT with and without the addition of diagonal matrix to the weighting matrix, and for comparison, we also introduce another special case of OMA, and we call it revised WKLT (RWKLT), which considers both the color matching functions of human observer and the influence of a predetermined illuminant set in the weighting matrix. In order to utilize these transforms for spectral decorrelation of multispectral images, we adopt the following process: first, the spectral reflectance is estimated from the multispectral data by certain estimation method such as Wiener estimation, and the estimated spectral reflectance is transformed by different transforms, followed by JPEG2000 as the spatial compression scheme.

SPECTRAL TRANSFORMS FOR MULTISPECTRAL IMAGE COMPRESSION FOR BETTER COLOR REPRODUCIBILITY

Some spectral transforms for multispectral image compression in purpose of better color reproducibility have been proposed, including OMA, WKLT,[14] etc., which are shortly outlined in the Appendix, as well as the celebrated KLT. OMA is a general concept that incorporates a weighting matrix in KLT and WKLT is a special case of OMA, where in the weighting matrix of WKLT, the color matching functions of human observers are considered.

Besides OMA and WKLT, we also introduce a revised version of WKLT (RWKLT) in this section, which is another special case of OMA. RWKLT can consider the influence of a predetermined illuminant set as well as the color matching functions of human observer in its weighting matrix.

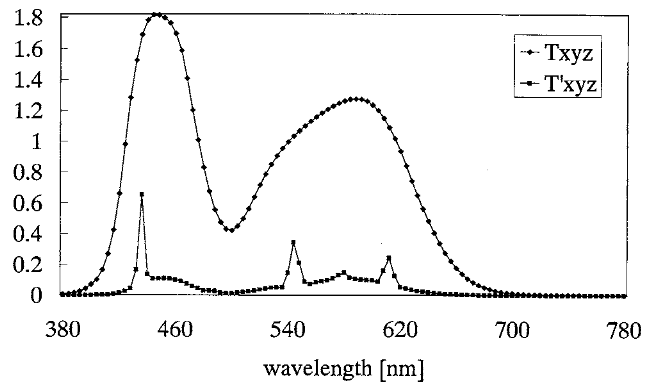

Figure 1. Diagonal coefficients for the weighting matrices of WKLT and RWKLT.

As stated in the Appendix, WKLT is based on the assumption that the number of illuminants L is towards infinite so that different kinds of illuminants can be considered as independently and identically distributed at each wavelength. In practice, we can limit the set of illuminants that are frequently used for real applications of color reproduction. In such cases, recalling the weighting matrix for WKLT:

$$\boldsymbol{W}_{\mathrm{WKLT}}^2 = \boldsymbol{T}_{XYZ}^2 = \boldsymbol{T}_X^2 + \boldsymbol{T}_Y^2 + \boldsymbol{T}_Z^2, \tag{1}$$

where $\boldsymbol{T}_X, \boldsymbol{T}_Y, \boldsymbol{T}_Z$ are diagonal matrices whose diagonal elements indicate the color matching functions of human observer, such as CIE 1931 XYZ color matching functions, it is reasonable to substitute $\boldsymbol{W}_{\mathrm{WKLT}}$ by $\boldsymbol{W}_{\mathrm{RWKLT}}$ to take the influence of the illuminants into consideration:

$$\boldsymbol{W}_{\mathrm{RWKLT}}^2 = \boldsymbol{T}'_{XYZ} = \boldsymbol{T}_X R T_X + \mathrm{T}_Y \boldsymbol{R} \boldsymbol{T}_Y + \boldsymbol{T}_Z \boldsymbol{R} \boldsymbol{T}_Z, \tag{2}$$

where

$$\boldsymbol{R} = \bar{\mathbf{E}}\bar{\mathbf{E}}^T. \tag{3}$$

Here we use the normalized illuminant set $\bar{\mathbf{E}} = (\bar{\mathbf{e}} | \bar{\mathbf{e}}_i = \mathbf{e}_i / \|\mathbf{e}_i\|)$, $i = 1, 2, \ldots, L$, to equalize the influence of different illuminants $\mathbf{e}_i (i = 1, 2, \ldots, L)$. In order to distinguish from WKLT, we call the transform that incorporates the weighting matrix of $\boldsymbol{W}_{\mathrm{RWKLT}}$ as RWKLT.

Figure 1 shows the diagonal values for the weighting matrices of WKLT and RWKLT, where the illuminant set used in RWKLT is shown in Fig. 2 and will be further demonstrated in the experimental section. It can be seen that the weighting matrices decrease at long visible wavelength for both WKLT and RWKLT by the influence of the spectral shape of the color matching function. In addition, we can also observe the effect of the predetermined illuminant set in the case of RWKLT. That the magnitudes for the weighting matrix of RWKLT are smaller compared to that of WKLT is caused by illumination normalization in RWKLT.

Besides, as OMA, WKLT, and RWKLT are all KLT based transforms, they are image-dependent and the pertinent statistics information of the image data is needed for the calculation of KLT vectors. In this paper, the correlation matrix

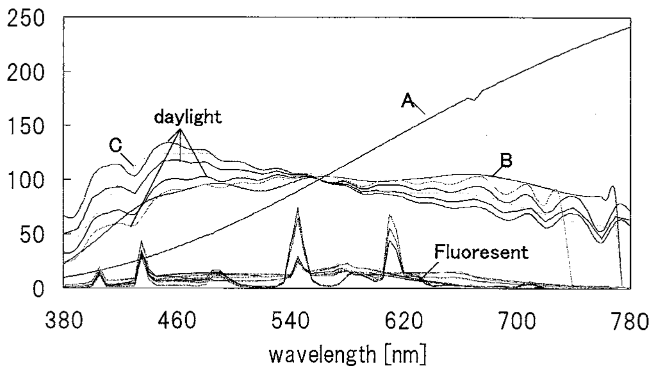

Figure 2. Spectral radiances of the illuminants that are used as the illuminant set for the weighting matrix of RWKLT.

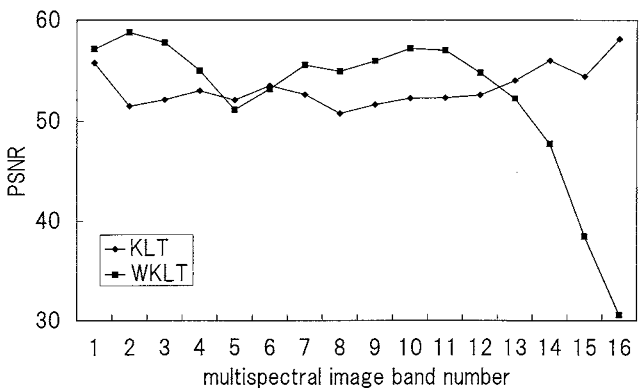

Figure 3. Comparison of PSNR results for each band image of a 16-band multispectral image using KLT and WKLT as the spectral transform. The horizontal axis indicates the multispectral image band number, which is in accordance to the spectral wavelength, the larger the number value, the longer central wavelength for the corresponding multispectral color filter.

that is used to obtain the basis functions of KLT is generated from the spectral reflectance, which is estimated from the original multispectral image. The image-independent scheme for the simplification of calculating the correlation matrix is our future issue.

ADDITION OF DIAGONAL MATRIX TO WEIGHTING MATRIX

WKLT and RWKLT based methods are superior in color reproducibility compared with KLT based multispectral image compression scheme.[8] However, the improvement in color accuracy is on the cost of poor spectral accuracy. Figure 3 compares the peak signal-to-noise ratio (PSNR) as the measurement for spectral accuracy for each band of a 16-band multispectral image, respectively, using KLT and WKLT based compression methods. We can observe the shape of the WKLT result is similar to the shape of the weighting matrix of WKLT in Fig. 1, where the magnitudes of diagonal elements of the weighting matrix are small in long wavelengths. When multiplied by such a weighting matrix, the spectral reflectance estimated from the multispectral image will also become small in the corresponding wavelengths. In the viewpoint of image compression, this process equals to quantize the spectral reflectance of the corresponding wavelength range by larger quantization step-sizes, which will result in bigger quantization error and degradation in spectral accuracy for the corresponding wavelengths range, as is shown in Fig. 3.

In order to improve the spectral accuracy, let us recall the cost function for KLT (in the Appendix), which aims to minimize the spectral error and we can take the weighting matrix for KLT as an identity matrix. Namely, the improvement of spectral accuracy in WKLT can be achieved by a compromise of WKLT and KLT. Thus we define a modified cost function to take both the colorimetric and spectral accuracies into consideration

$$\varepsilon = \|\boldsymbol{W}(\mathbf{f}-\hat{\mathbf{f}})\|^2 + \alpha^2\|\mathbf{f}-\hat{\mathbf{f}}\|^2, \tag{4}$$

Here, the first item $\boldsymbol{W}(\mathbf{f}-\hat{\mathbf{f}})$ is according to the colorimetric accuracy while the second item $(\mathbf{f}-\hat{\mathbf{f}})$ to spectral accuracy reproduction and α determines the balance of colorimetric and spectral accuracies. We can further write Eq. (4) into

$$\varepsilon \geqslant \tfrac{1}{2}(\|\boldsymbol{W}(\mathbf{f}-\hat{\mathbf{f}}) + \alpha(\mathbf{f}-\hat{\mathbf{f}})\|^2) = \tfrac{1}{2}(\|(\boldsymbol{W}+\alpha\mathbf{I})(\mathbf{f}-\hat{\mathbf{f}})\|^2), \tag{5}$$

which means that the minimization of the cost function in Eq. (A1) can be realized by substituting $\boldsymbol{W}$ in Eq. (A4) by $\boldsymbol{W}+\alpha\mathbf{I}$. Therefore, it can be said that by adding a scalar multiple of an identity matrix to the weighting matrices of WKLT or RWKLT, the spectral accuracy can be taken into account as well as the colorimetric accuracy. In this case, the near zero values can be lifted up and thus the quantization errors can be reduced in the corresponding reconstructed multispectral image channels. At the same time, the feature of weighting matrices for WKLT and RWKLT can also be preserved if the scalar α is small and properly chosen.

The magnitude of the scalar α can be determined according to the different applications of the multispectral image and the intent for compression system design. Too large value of α will diminish the effects of the weighting matrices for WKLT and RWKLT and cause colorimetric degradation, while too small α will result in little improvements for spectral accuracy.

Let us rewrite Eq. (5) as

$$\varepsilon \propto \{\|\boldsymbol{W}\|^2 + \alpha^2\}\|\Delta\mathbf{f}\|^2, \tag{6}$$

where $\Delta\mathbf{f}=\mathbf{f}-\hat{\mathbf{f}}$ and if $\Delta\mathbf{f}$ is constant for all wavelength, $\|\Delta\mathbf{f}\|^2$ can be written as

$$\|\Delta\mathbf{f}\|^2 = N\cdot\Delta\varepsilon_1^2, \tag{7}$$

where N refers to the number of spectral samples in the wavelength range of the narrow visual band (380–780 nm) of the spectral data for color reproduction and $\Delta\varepsilon_1$ is the difference between $\mathbf{f}$ and $\hat{\mathbf{f}}$ under a single wavelength. Then Eq. (6) can be written as

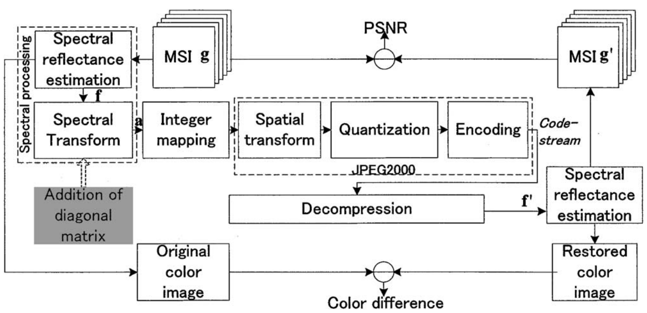

Figure 4. Multispectral compression framework and evaluation measurements.

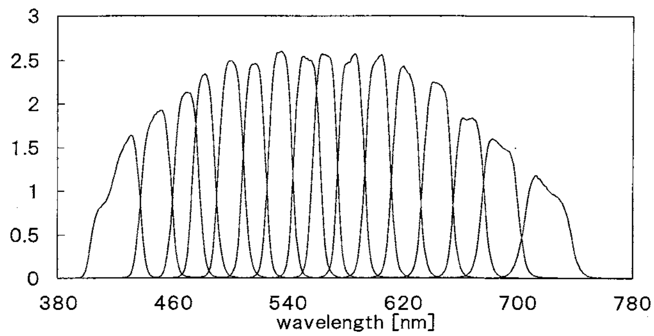

Figure 5. Spectral sensitivity of the 16-band multispectral camera used in experiments.

$$\varepsilon \propto \{\|\boldsymbol{W}\|^2 + \alpha^2\}\|\Delta \mathbf{f}\|^2 = \{\|\boldsymbol{W}\|^2 + \alpha^2\}N\Delta\varepsilon_1^2. \tag{8}$$

From Eq. (8), we can find the weighting factor α^2 is inversely proportional to the wavelength range of the spectral data N when ε is constant. That is to say, α is inversely proportional to the square root of the range of spectral data

$$\alpha_{\mathrm{WKLT}} = 1/\sqrt{N} = 1/\sqrt{\text{wavelength range of the spectral data}}. \tag{9}$$

For RWKLT, the influence of the illuminant set is also considered, along with the number of samples in of the range of the spectral data. α_{RWKLT} is defined as

$$\alpha_{\mathrm{RWKLT}} = 1/\sqrt{\|\mathbf{I}_k\| L}, \tag{10}$$

where L is the number of the illuminants used in the weighting matrix of RWKLT and k is the dimension of the spectral data $\mathbf{f}$. Here, the functionality of $\|\mathbf{I}_k\|$ is the same as that of N in Eq. (9).

COMPRESSION SCHEME

In order to implement the multispectral image compression based on the proposed method to preserve both colorimetric and spectral accuracy, in this section, we will introduce the total compression scheme, which is shown in Fig. 4: First, the spectral reflectance $\mathbf{f}$ is obtained by Wiener estimation pixel by pixel from the original multispectral image $\mathbf{g}$, then spectral transform is performed on the estimated spectral reflectance. These spectral processes can be done by vector matrix product. Suppose the numbers of channels in the multispectral image $\mathbf{g}$ and the spectral reflectance $\mathbf{f}$ are j and k, respectively, where the rank of $\mathbf{f}$ is j, and $k \times j$ matrix $\boldsymbol{M}$ represents the Wiener estimation matrix, and $k \times k$ matrix $\boldsymbol{R}$ with the rank j is the spectral transform matrix, then the spectral transform coefficient vector $\mathbf{a}$ with the size k and rank j can be expressed by

$$\mathbf{a} = \boldsymbol{R} \cdot \mathbf{f} = \boldsymbol{R} \cdot \boldsymbol{M} \cdot \mathbf{g}. \tag{11}$$

The proposed spectral transform method can be used in combination with different spatial compression schemes. Among them, JPEG2000 is suitable for multispectral image compression, because it can deal with both gray-scale and multichannel images. Meanwhile, JPEG2000 can integrate both lossless and lossy compressions under the same framework.[15] Furthermore, although it is not the definitive reason to choose the format, the supplementary information needed for the color reproduction can be stored in metadata in JPEG2000 format.[16] All these merits of JPEG2000 make it a good candidate to serve as the spatial compression scheme in our multispectral compression system.

For the implementation of JPEG2000, the software LuraWave.jp2 by LuraTech company is used.[17] Because the spectral transform coefficients are all real numbers, we must quantize them into integers for the input of JPEG2000. The following quantization method is used in the experiment.[8]

Suppose a_{abs} be the maximum of the absolute value in all transform coefficient channels, the coefficients inside the interval $(-a_{\mathrm{abs}}, a_{\mathrm{abs}})$ will be linearly quantized to the q-bit integer values by

$$a' = \left\lfloor \frac{a - a_{\mathrm{abs}}}{2a_{\mathrm{abs}}} \right\rfloor (2^q - 1), \tag{12}$$

where q is the bit depth of the transformed coefficient and the operation $\lfloor\ \rfloor$ denotes to round the real number towards the nearest integer to the minus infinity.

EXPERIMENT

Three multispectral images are used in the experiments, which are captured by a multispectral camera with 16 narrow band color filters.[2] The spectral sensitivities of the multispectral camera color filters are shown in Fig. 5. Figure 6 shows one band for each of the three multispectral images, respectively, all in the color filter central wavelength of 550 nm. Each band image consists of 512×512 pixels with 16-bit dynamic resolution, which is downsampled from the original 1024×1024 pixels' image. For convenience of demonstration, we name the three multispectral images in Fig. 6 toy, scarf, and flowers, respectively.

The illuminant set used in RWKLT is shown in Fig. 2, altogether 19 kinds of illuminants, including CIE A, B, C, and 4 kinds of daylight with different color temperature (denoted by D50, D55, D65, and D75) and a set of fluorescent (denoted by F1-F12). We assume the viewing illuminant for the experiments is one of CIE D65, F2 and FLAT, where FLAT indicates the spectral power is evenly distributed along

(a)

(b)

(c)

Figure 6. One band image for each multispectral image used in the experiments with 550 nm of central wavelength of the color filter. For notation, we name them (a) toy, (b) scarf, and (c) flowers.

wavelength. Here D65 and F2 are inside the illuminant set of RWKLT, while FLAT is not included in the predetermined illuminant set.

For experimental evaluation, we use PSNR as the measurement for spectral accuracy, which is expressed by

$$\mathrm{PSNR} = 20 \log \frac{2^b - 1}{\|\mathbf{g} - \hat{\mathbf{g}}\|}, \tag{13}$$

where $\mathbf{g}$ and $\hat{\mathbf{g}}$ denote the original and reconstructed multispectral images, respectively, and b means the bit-depth of the multispectral pixels. And for the evaluation of color reproducibility, CIE 1931 L*a*b* color difference under a certain illuminant is used, which is denoted by $\Delta E_{ab}*$:

$$\Delta E^*_{ab} = [(\Delta L^*)^2 + (\Delta a^*)^2 + (\Delta b^*)^2]^{1/2}, \tag{14}$$

where ΔL^*, Δa^*, and Δb^* represent the differences of the CIE L*a*b* color images restored from the original and reconstructed multispectral images.

Moreover, in this paper, the compression ratio is defined as

$$\mathrm{CR} = \frac{\text{compressed data size}}{\text{original data size}}. \tag{15}$$

DETERMINATION OF THE MAGNITUDE OF THE DIAGONAL MATRIX

In the experiments, we examine the effectiveness of the proposed method to determine the scalar α, which indicates the magnitude of the diagonal matrix that are added to the weighting matrices of WKLT and RWKLT. Figure 7 shows the relationship between PSNR and the magnitude of the diagonal matrix added to the weighting matrix of WKLT and RWKLT for image flowers under various compression ratios. Figure 8 shows the relationship between average CIE L*a*b* color differences and the magnitudes of the diagonal matrix added to the weighting matrix of WKLT and RWKLT for image flowers under different illuminants when CR=0.05. α_{WKLT} and α_{RWKLT} in the figures are corresponding to the magnitudes for the diagonal matrices that are determined by Eqs. (9) and (10). We can also get similar results from the experiments of the other two multispectral images. From these results, we can notice that in both cases of WKLT and RWKLT, the PSNR always increase with the increase of α. More specifically, PSNR is very sensitive and increase a great deal when $\alpha \leqslant \alpha_{\mathrm{WKLT}}(\alpha_{\mathrm{RWKLT}})$, while $\alpha > \alpha_{\mathrm{WKLT}}(\alpha_{\mathrm{RWKLT}})$, PSNR becomes not very sensitive to the variance of α. In the case of color difference, the results in Fig. 8 show that the color difference is much more sensitive to the increase of α and when $\alpha > \alpha_{\mathrm{WKLT}}(\alpha_{\mathrm{RWKLT}})$, although PSNR still increases a little in Fig. 7, the color differences will get worse rapidly. This means the calculated magnitude of the diagonal matrix for WKLT and RWKLT by Eqs. (9) and (10) can reach a good balance between spectral and colorimetric accuracies.

Moreover, the tendencies of PSNR and color difference results in Figs. 8 and 9 appear to be similar for various

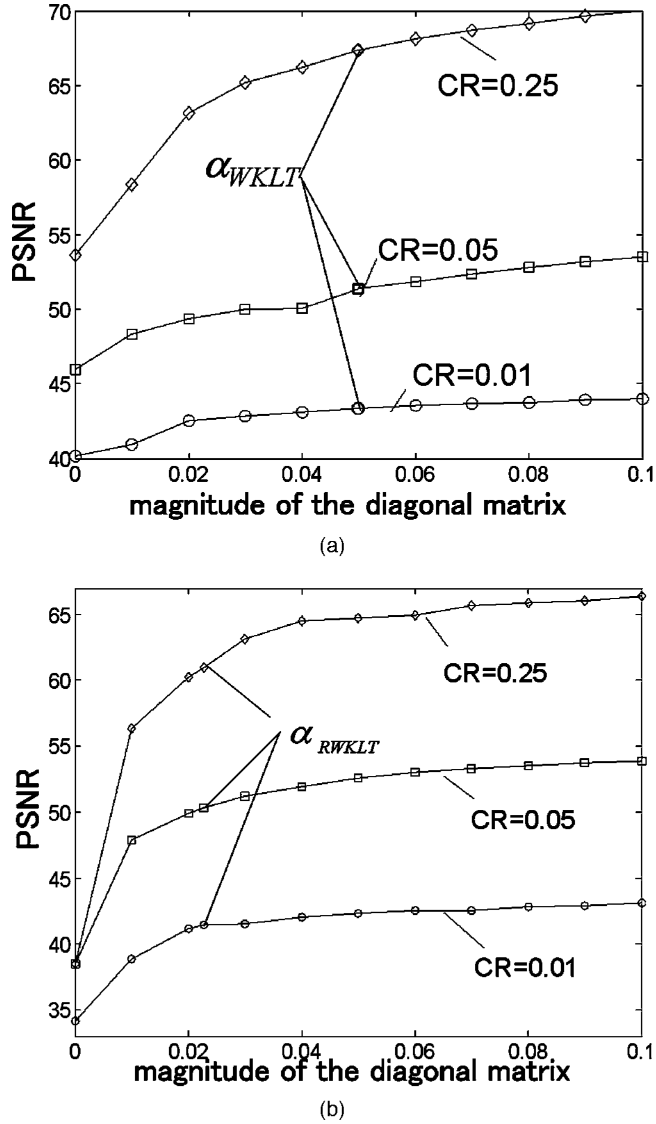

Figure 7. The magnitude of the diagonal matrix that are added to the weighting matrix of (a) WKLT, (b) RWKLT vs PSNR under different compression ratio for image flowers. The specified magnitudes are determined by Eqs. (9) and (10).

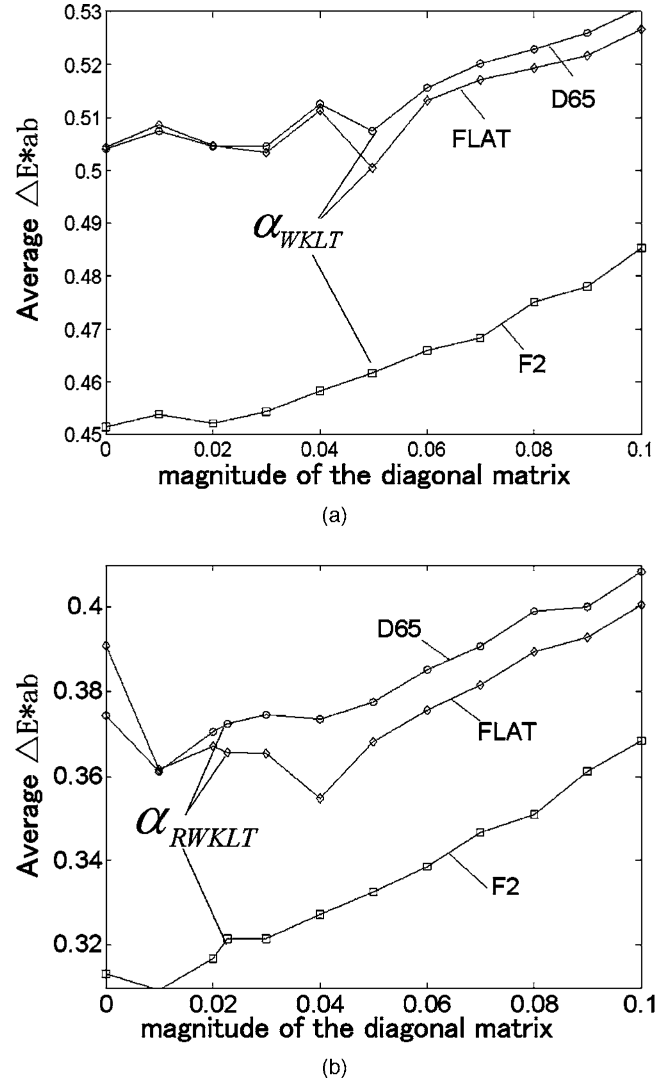

Figure 8. The magnitude of the diagonal matrix that are added to the weighting matrix of (a) WKLT (b) RWKLT vs average CIE L*a*b* color differences under different illuminants when CR=0.05. The specified magnitudes are determined by Eqs. (9) and (10).

magnitude of α under different illuminants for both WKLT and WRKLT and a small deviate of α will not change the colorimetric results very much. That means the regularized parameter α is robust for various illuminants, transforms, as well as a mis-specified parameter α.

COMPARISON OF WKLT AND RWKLT WITH THE ADDITION OF DIAGONAL MATRIX

In this section, we will compare the performance of WKLT and RWKLT with the addition of diagonal matrix to the weighting matrix as the spectral transform for multispectral image compression. For comparison purpose, we will use KLT, WKLT (with and without the addition of diagonal matrix), and RWKLT (with and without the addition of diagonal matrix) as the spectral transforms in the experiments. Moreover, we will use Eqs. (9) and (10) for the determination of the magnitudes for the diagonal matrices.

Figure 9 is a comparison between the first four analysis vectors for KLT, WKLT, and RWKLT, respectively, which are obtained from the spectral reflectance estimation of multispectral image toy. We can see compared with the vectors for KLT, WKLT, and RWKLT can reflect the influence of the spectral shape of the color matching function, and RWKLT contains the information of the predetermined illuminant set.

In Fig. 10, PSNR versus different compression ratio is shown as the measurement of the spectral accuracy of the reconstructed multispectral image using different spectral transforms As the measurements for color reproducibility, the average and the maximum $E[a^*b]$ versus the compression ratio under viewing illuminant F2 are shown in Fig. 11. In those results, test image is flowers. From the results, it is confirmed that in the aspect of PSNR, adding a suitable diagonal matrix to the weighting matrix of WKLT or RWKLT can greatly improve the spectral accuracy; And in

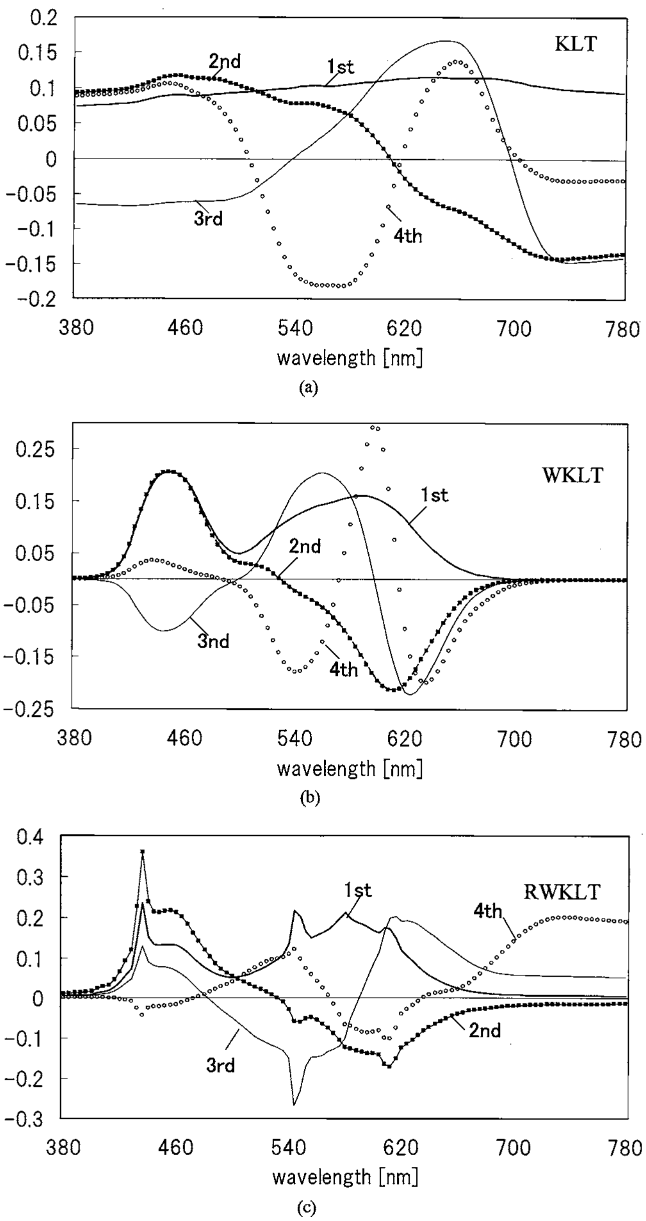

Figure 9. First four analysis vectors of KLT, WKLT, and RWKLT obtained from the spectral reflectance estimated from multispectral image toy.

the aspect of colorimetric error, the results for WKLT or RWKLT methods, with and without the addition of the diagonal matrix, are almost the same in a wide range of compression ratio, which in turn proves the effectiveness of our proposed method to determine the magnitude of the diagonal matrix. Specifically, the results for RWKLT based method can get the best color accuracy results in a large range of compression ratio, except at low bit rates. That is caused by the normalization for the illuminants used in the weighting matrix of RWKLT, which reduced the dynamic range of the RWKLT coefficients, thus made them more sensitive to the quantization errors at low bit rates.

The results of the other two multispectral images under various illuminants are summarized in Tables I and II, Table I shows the results for image scarf under illuminant F2 while

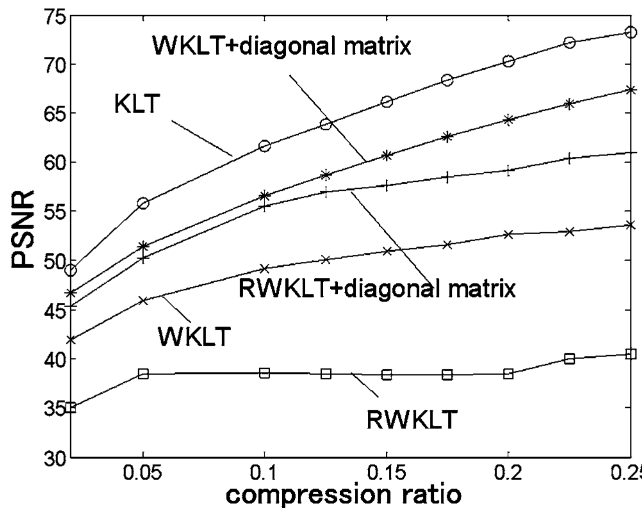

Figure 10. Comparison for PSNR using different spectral transforms for image flowers.

Table II is for image toy under illuminant D65. From those results, we can conclude that although there are some differences according to different test images or viewing illuminants, the tendency of the results are almost the same.

Moreover, still in the case of RWKLT, adding a suitable diagonal matrix to the weighting matrix has good generalization ability even when the viewing illuminant is not included in the presumed illuminant set. Figure 12 shows an

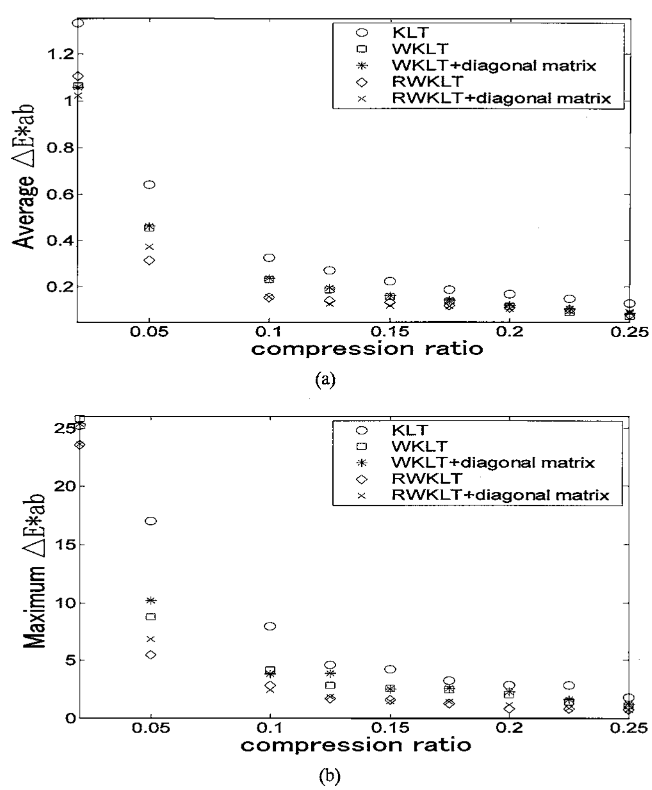

Figure 11. Comparison for color difference using different spectral transforms for image flowers under illuminant F2 (a) average $E[a*b]$ (b) maximum $E[a*b]$.

Table I. Results for image scarf under illuminant F2.

CR		0.01	0.05	0.25
KLT	PSNR	41.10	52.48	71.63
	ave $E[a^*b]$	2.67	0.77	0.14
	max $E[a^*b]$	51.16	15.56	1.89
WKLT	PSNR	36.20	40.77	51.04
	ave $E[a^*b]$	2.16	0.48	0.09
	max $E[a^*b]$	36.65	15.41	1.24
WKLT with diagonal matrix	PSNR	39.43	48.25	65.57
	ave $E[a^*b]$	2.14	0.50	0.10
	max $E[a^*b]$	37.5	15.00	1.45
RWKLT	PSNR	31.20	40.32	50.98
	ave $E[a^*b]$	2.41	0.32	0.03
	max $E[a^*b]$	48.54	10.65	0.50
RWKLT with diagonal matrix	PSNR	37.00	47.85	58.74
	ave $E[a^*b]$	2.49	0.34	0.03
	max $E[a^*b]$	52.09	10.77	0.49

Table II. Results for image toy under illuminant D65.

CR		0.01	0.05	0.25
KLT	PSNR	42.48	52.95	71.83
	ave $E[a^*b]$	3.42	1.11	0.18
	max $E[a^*b]$	49.07	20.41	1.91
WKLT	PSNR	34.40	41.72	50.14
	ave $E[a^*b]$	2.64	0.71	0.13
	max $E[a^*b]$	40.54	13.26	1.53
WKLT with diagonal matrix	PSNR	40.99	48.93	65.84
	ave $E[a^*b]$	2.65	0.71	0.13
	max $E[a^*b]$	39.29	10.20	1.67
RWKLT	PSNR	33.45	41.25	49.86
	ave $E[a^*b]$	2.98	0.49	0.05
	max $E[a^*b]$	46.56	8.28	0.72
RWKLT with diagonal matrix	PSNR	38.13	48.74	56.66
	ave $E[a^*b]$	3.01	0.52	0.06
	max $E[a^*b]$	45.40	8.42	0.70

example for image flowers, when the viewing illuminant is FLAT, which is not included in the presumed illuminant set for RWKLT. In this example, we can observe that RWKLT without the addition of diagonal matrix will have little effect to colorimetric error reduction at high bit rates. The degradation of color reproducibility of RWKLT is related to the number and the kinds of illuminants that are used in the

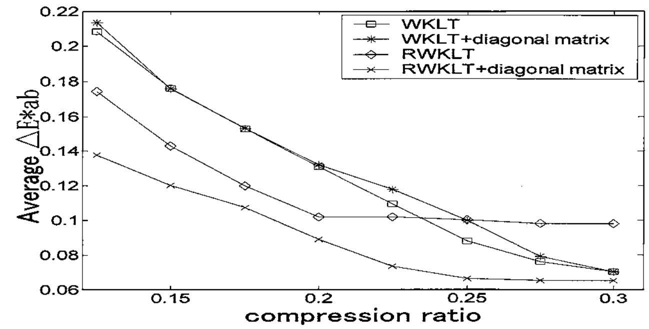

(a)

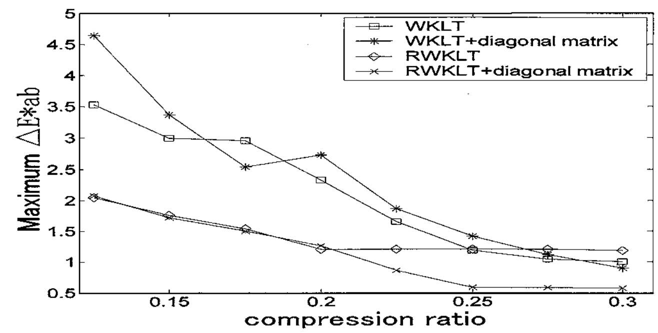

(b)

Figure 12. Comparison for color difference using RWKLT with and without the addition of diagonal matrix when the viewing illuminant is FLAT, which is not included in the presumed illuminant set for RWKLT. (a) Average $E[a*b]$ (b) maximum $E[a*b]$.

illuminant set, and the similarity of the illuminant to those in the illuminant set. This is similar to linear pattern matching filter design, where the filter is sometimes designed from a limited training set. Then if the training set is ill suited and cannot represent a large range of dataset, the filter may be only optimized to the training set, while for other test set, the performance will get worse. The addition of diagonal matrix to the weighting matrix of RWKLT can improve such phenomenon to some extent, as is shown also in Fig. 12, both the average and the maximum color difference are reduced in high bit rate range when the diagonal matrix is added to the weighting matrix of RWKLT.

CONCLUSION AND DISCUSSION

The purpose of this paper is to propose a multispectral image compression method for high fidelity color reproducibility with spectral accuracy preservation. We add a diagonal matrix to the weighting matrix of WKLT and RWKLT and determine the magnitude of the diagonal matrix by a novel cost function. Experimental results that are performed on three 16-channel multispectral images shown the advantage of adding a suitable diagonal matrix, where spectral accuracy is improved without substantial loss of color reproducibility. Moreover, the addition of the diagonal matrix has generalization effect for RWKLT in the case when the viewing illuminant is out of the predetermined illuminant set. Furthermore, it is valuable to integrate the propose method to JPEG2000 for the compression of multispectral images and the fact that fixed magnitude of the diagonal matrix works well for various multispectral images are also fine for practical use.

REFERENCES

[1] R. S. Berns, F. H. Imai, P. D. Burns, and D. Tzeng, "Multispectral-based color reproduction research at the Munsell color science laboratory", IEEE Trans. Image Process. **3409**, 14 (1998).
[2] M. Yamaguchi, T. Teraji, K. Ohsawa, T. Uchiyama, H. Motomura, Y. Murakami, and N. Ohyama, "Color image reproduction based on the multispectral and multiprimary imaging; experimental evaluation", in Proc. SPIE **4663**, 15 (2002).
[3] J. Mielikainen and A. Kaarna, "Improved back end for integer PCA and wavelet transforms for lossless compression of multispectral images", *Proc. IEEE Pattern Recognition* **2**, 257 (2002).
[4] A. Kaarna, P. Zemcik, H. Kalviainen, and J. Parkkinenm, "Compression of multispectral remote sensing images using clustering and spectral reduction", IEEE Trans. Geosci. Remote Sens. **GE–38**, 1073 (2000).
[5] B. R. Epstein, R. Hingorani, and J. M. Shapiro, "Multispectral image compression by wavelet/karhunen-loeve transformation", in *Proc. Geoscience and Remote Sensing Symposium, IGARSS'92*, 672 (1992).
[6] Y. Murakami, H. Manabe, T. Obi, M. Yamaguchi, and N. Ohyama, "Multispectral image compression for color reproduction; weighted KLT and adaptive quantization based on visual color perception", in *Proc. IS&T/SID 9th Color Imaging Conference* (IS&T, Springfield, VA, 2001) p. 68.
[7] D. H. Marimont and B. A. Wandell, "Linear models of surface and illuminant spectra", J. Opt. Soc. Am. A **11**, 1905 (1992).
[8] R. Mase, Y. Kawasaki, Y. Murakami, T. Obi, M. Yamaguchi, and N. Ohyama, "Multispectral image compression for high quality color reproduction using JPEG2000", in Proc. SPIE **5308**, 808 (2004).
[9] X. L. Tao and H. E. Michel, "Classification of multispectral satellite image data using improved NRBF neural networks", in Proc. SPIE **5267**, 311 (2003).
[10] R. Ramanath and W. E. Snyder, "Eigenviews for object recognition in multispectral imaging systems", *32nd Applied Imagery Pattern Recognition Workshop (AIPR'03)*, 33 (2003).
[11] S. Tominaga, "Material identification via multi-Spectral imaging and its application to circuit boards", *Proc. IS&T/SID 10th Color Imaging Conference* (IS&T, Springfield, VA, 2002) p. 217.
[12] J. Barros, J. French, W. Martin, P. Kelly, and J. M. White, "Indexing multispectral images for content-based retrieval," in *Proceedings of the 23rd AIPR Workshop on Image and Information Systems: Applications and Opportunities* (1994).
[13] H. Kim, B. Kang, G. Han, J. Kim, C. Yoon, and M. Cho, "A method of printer modeling with the spectral reflectance curves using error back propagation," *Systems, Man, and Cybernetics, 1998, IEEE Int. Conf.*, **2**, 1796 (1998).
[14] Y. Murakami, H. Manabe, T. Obi, M. Yamaguchi, and N. Ohyama, "Comparative evaluation of spectral transforms for multispectral image coding in terms of color degradation," Opt. Rev. **11**, 76 (2004).
[15] David S. Taubman and Michael W. Marcellin, *JPEG2000, Image compression fundamentals, standards, and practice*, 2nd ed. (Kluwer, Dordrecht, 2002).
[16] WC3 Recommendation. Extensible markup language (XML) 10, February 1998 (2nd ed., October 2000).
[17] http://www.jpeg.org/JPEG2000.

APPENDIX

In the Appendix, we will briefly introduce three spectral transforms for multispectral image compression, where the celebrated KLT is used for spectral accuracy reproduction and one mode analysis (OMA) and weighted KLT (WKLT) are proposed for better color reproducibility purpose.

KLT

KLT aims to minimize the error defined by

$$\varepsilon_{\mathrm{KLT}} = \langle \|\mathbf{f} - \hat{\mathbf{f}}\| \rangle, \tag{A1}$$

where $\mathbf{f}$ and $\hat{\mathbf{f}}$ denote the k-dimensional vector representations of the spectral reflectance estimated from the j-channel original and reconstructed multispectral images. KLT for $\mathbf{f}$ can be expressed by

$$\mathbf{A} = \mathbf{Pf}, \tag{A2}$$

where $\mathbf{A}$ is the j-dimensional vector of the KLT coefficient, and the transformation matrix

$$\boldsymbol{P} = (\mathbf{p}_1, \mathbf{p}_2, \ldots, \mathbf{p}_j)^T, \tag{A3}$$

contains KLT analysis vectors $\mathbf{p}_i (i=1,2,\ldots j)$, which are the eigenvectors of the correlation matrix $\boldsymbol{ff}^T$ and the rank of the correlation matrix is j.

OMA

OMA incorporates an $k \times k$ weighting matrix $\boldsymbol{W}$ to the spectral reflectance and is proposed to minimize the following error

$$\varepsilon_{\mathrm{OMA}} = \langle \|\boldsymbol{W}(\mathbf{f} - \hat{\mathbf{f}})\|^2 \rangle. \tag{A4}$$

OMA can be expressed as:

$$\mathbf{B} = \boldsymbol{Q}(\boldsymbol{W}\mathbf{f}), \tag{A5}$$

where $\mathbf{B}$ is the j-dimensional vector of the OMA coefficient, and the transformation matrix $\boldsymbol{Q} = (\mathbf{q}_1, \mathbf{q}_2, \ldots \mathbf{q}_j)$ includes the eigenvector $\mathbf{q}_i (i=1,2,\ldots,j)$ of the matrix $\boldsymbol{W}\langle \mathbf{ff}^T \rangle \boldsymbol{W}^T$.

WKLT

OMA is a general model and the weighting matrix $\boldsymbol{W}$ can be defined for different purposes. WKLT is a special case of OMA proposed by Murakami that aims to minimize the error[7]

$$\begin{aligned}\varepsilon_{\mathrm{WKLT}} &= \langle \|\boldsymbol{W}_{\mathrm{WKLT}}(\mathbf{f} - \hat{\mathbf{f}})\|^2 \rangle = \langle (\mathbf{f} - \hat{\mathbf{f}})^T \boldsymbol{W}_{\mathrm{WKLT}}^T \boldsymbol{W}_{\mathrm{WKLT}} (\mathbf{f} - \hat{\mathbf{f}}) \rangle \\ &= \langle (\mathbf{f} - \hat{\mathbf{f}})^T (\boldsymbol{T}_X \boldsymbol{E}\boldsymbol{E}^T \boldsymbol{T}_X + \boldsymbol{T}_Y \mathbf{E}\mathbf{E}^T \boldsymbol{T}_Y + \boldsymbol{T}_Z \boldsymbol{E}\boldsymbol{E}^T \boldsymbol{T}_Z)(\mathbf{f} - \hat{\mathbf{f}}) \rangle,\end{aligned} \tag{A6}$$

where $\boldsymbol{T}_X, \boldsymbol{T}_Y, \boldsymbol{T}_Z$ are diagonal matrices whose diagonal elements indicate the color matching functions of human observer, such as CIE 1931 *XYZ* color matching functions and the matrix $\boldsymbol{E} = (\mathbf{e}_1, \mathbf{e}_2, \ldots, \mathbf{e}_L)$ represents the spectral radiations of L kinds of illuminants $\mathbf{e}_i (i=1,2,\ldots,L)$. In order to simplify the weighting matrix, WKLT assumes that L gets closer to infinite and the correlation matrix of illuminants $\boldsymbol{EE}^T$ is approximated by a scalar multiple of an identity matrix. Thus the weighting matrix can be simplified as

$$\boldsymbol{W}_{\mathrm{WKLT}}^2 = \boldsymbol{T}_{XYZ}^2 = \boldsymbol{T}_X^2 + \boldsymbol{T}_Y^2 + \boldsymbol{T}_Z^2. \tag{A7}$$